

# Effect of nanometer TiC coated diamond on the strength and thermal conductivity of diamond/Al composites



X.Y. Liu <sup>a, b</sup>, W.G. Wang <sup>c</sup>, D. Wang <sup>c</sup>, D.R. Ni <sup>c</sup>, L.Q. Chen <sup>a</sup>, Z.Y. Ma <sup>c, \*</sup>

<sup>a</sup> State Key Laboratory of Rolling and Automation, Northeastern University, Shenyang 110819, China

<sup>b</sup> College of Science, Shenyang Ligong University, Shenyang 110159, China

<sup>c</sup> Shenyang National Laboratory for Materials Science, Institute of Metal Research, Chinese Academy of Sciences, Shenyang 110016, China

## HIGHLIGHTS

- 10 nm thick TiC coating improved the wettability between diamond and Al matrix.
- The density of TiC-coated diamond/6061Al reached 99.6% of theoretical value.
- TiC coating resulted in 35% increase in the bending strength of diamond/6061Al.
- TiC coating resulted in 13.4% increase in the thermal conductance of diamond/6061Al.
- Massive gap of phonon velocity between diamond and Al affects thermal conductance.

## ARTICLE INFO

### Article history:

Received 22 February 2016

Received in revised form

3 July 2016

Accepted 10 July 2016

Available online 16 July 2016

### Keywords:

Composite materials

Interfaces

Mechanical properties

Thermal conductivity

Powder metallurgy

## ABSTRACT

50 vol% TiC-coated diamond particles reinforced 6061Al (TiC@diamond/6061Al) composites were fabricated by using powder metallurgy method. The TiC coating 10 nm in thickness on the diamond particles could improve the wettability and increase the bonding between the diamond and Al matrix. The density of the TiC@diamond/6061Al composites reached 99.6% of the theoretical density, which was much higher than that (96.7%) of the composite using the diamond without the TiC layer (Diamond/6061Al). The bending strength of the TiC@diamond/6061Al was 396 MPa, 35% higher than that of the Diamond/6061Al. However, the thermal conductance of the TiC@diamond/6061Al was only 13.4% higher than that of the Diamond/6061Al. This indicates that the massive gap in phonon velocity between diamond and Al, not the pores in the composites, was the dominant factor in the thermal conductance of the diamond particles reinforced Al composites.

© 2016 Elsevier B.V. All rights reserved.

## 1. Introduction

The power densities of electronic chips has increased dramatically in the past decade, as the extent of electronic chips integration increased [1,2]. To prevent large temperature rises as a result of these high power densities, the heat should be removed from the chips immediately upon generation. One common technique is the usage of a heat sink, made from materials with a high thermal conductivity (TC) to dissipate the heat from the chips. In addition, these materials also have low thermal expansion coefficients and good resistance to thermal fatigue.

Metal matrix composites (MMC), whose properties could be

tailored by adding appropriate reinforcements, had important advantages as heat sink materials [3]. The typical MMC heat sink materials such as Cu/Mo, Cu/W or Al/SiC with TCs of ~200 W/mK have been widely used in electronic devices [4,5]. However, the TCs of these traditional heat sink materials cannot sufficiently satisfy the exponential growth of power density in the electronic packaging field. Therefore, new sink materials with high TCs are in urgent demand.

Synthetic diamonds with thermal conductivities in the range of 1200–2000 W/mK are considered perfect reinforcements in the MMC for the next generation of heat sink materials [6]. In the past few decades, the diamond/Al composites have drawn much attention from both scientific and industrial communities due to their low density and good conduction properties [7–10]. The typical manufacturing methods of diamond/Al composites are liquid infiltration and powder metallurgy (PM) [8,11]. Even in the

\* Corresponding author.

E-mail address: [zyma@imr.ac.cn](mailto:zyma@imr.ac.cn) (Z.Y. Ma).

PM process, the occurrence of Al liquid was unavoidable during the manufacturing process [12]. The poor wettability and weak interface bonding between diamond and Al results in voids that are easily formed on the interface during the solidification process.

Schobel et al. [13] observed the formation of large irregularly shaped voids ( $\sim 0.7 \mu\text{m}^3$ ) in 60 vol% diamond/AlSi7 composite at eutectic solidification temperature by in-situ high resolution synchrotron tomography. These voids remained practically unchanged in shape and volume fraction during further cooling to room temperature. Therefore, in the earlier reports, high values of TC were not achieved in the diamond/Al composites [8,14,15].

It has been shown that gas pressure infiltration methods could avoid the formation of the pores effectively [16], and the TC of the resultant diamond/Al composites could reach up to 763 W/mK when using large monocrystalline diamond particles (150–178  $\mu\text{m}$ ) [16]. Usually, large diamond particles (more than 100  $\mu\text{m}$ ) should be used for the gas pressure infiltration process [15,16]. The large size of the diamond particles could increase the TC of the composites, but also causes extreme difficulties in machining the composites.

Modification of the surfaces of diamond particles by plating carbides is an effective way to improve the wettability and interface bonding between diamond and Al, thereby increasing the TC of the composites. In the past few years, various elements, such as Ti, Cr and W, were attempted to form the carbide coatings on diamond [17–20]. For example, a 0.5 mm-thick Ti coating on diamond resulted in a TC improvement from 325 to 491 W/mK for 50 vol% diamond/Al composites [21]. However, it is still much lower than the theoretical value of TC. Most researchers [17] attributed this phenomenon to the carbides layer itself. Some investigations [19] indicated that minimizing the thickness of a carbides layer with high TC could reduce the thermal boundary resistance between diamond and Al, and therefore, increase the TC of the composites.

However, the carbides, such as carbides of W and Cr, readily react with the Al matrix at high temperature. Even the TiC, which is considered to react with Al alloys hardly, also reacted easily with molten aluminum alloy at temperatures up to 720 °C [22]. Most reported carbides coated diamond/Al composites were prepared by the liquid infiltration process. However, the interface between the diamond and Al in these composites has never been observed. It is not clear whether the carbides react with Al matrix in the material preparation process and whether the TC increment of the composites is due to the carbide layers on the interface.

In this study, diamond particles with nanometer scale TiC coating was used to prepare the diamond/Al composite. For machining the sample easily, anomalous diamond particles with small sizes of 40–50  $\mu\text{m}$  were used. The aim of this study is to elucidate the interface structure between the diamond and Al in the TiC-coated diamond/Al composite and to clarify the key factors influencing the TC of the composites.

## 2. Experimental

The anomalous diamond (40–50  $\mu\text{m}$ , Type HWD40, Henan Huanghe Whirlwind International Co. Ltd., China), which was obtained by crashing the synthetic type Ib diamond, was used. The nitrogen content of the diamond was determined by analysis of its gaseous combustion product to be 100 ppm. Based on the data of Yamamoto [6], the intrinsic thermal conductivity of the diamond in this work was assumed to be 1800 W/mK.

The TiC coating on the diamond particles was fabricated by a sol-gel method.  $\text{TiO}_2$  sol was prepared using tetrabutyl titanate ( $\text{Ti}(\text{OC}_4\text{H}_9)_4$ ) as a precursor, anhydrous ethanol as a solvent, acetylacetone as a chelating agent, and nitric acid as an inhibitor. The volume ratio of tetrabutyl titanate, anhydrous ethanol, deionized

water, and acetylacetone was 1:9:0.7:0.15. Firstly, deionized water and 1/3 of the anhydrous ethanol were mixed, and the pH value of solution was adjusted to 3.0 with nitric acid. The obtained solution was denoted as solution A. Tetrabutyl titanate and acetylacetone were added to the rest of anhydrous ethanol, and solution B was obtained. Under magnetic stirring, solution A was slowly instilled into solution B to obtain a uniform and transparent sol. The diamond particles were stirred in the sol for 5 min and dried at room temperature for 2 days. Finally, the diamond particles were heated up to 1450 °C for 2 h in a vacuum furnace with a vacuum less than  $1.0 \times 10^{-1}$  Pa.

The 50 vol% diamond/6061Al composites were fabricated by the PM technique. The 6061Al (Al–Mg–Si) powders with a size of 50  $\mu\text{m}$  were used as the matrix. First, the Al alloy powders and diamond powders were blended and cold compacted. Then, the cold consolidated green billets were vacuum pressed at 100 MPa, producing the composite samples 50 mm in diameter and 50 mm in height. The composite reinforced by the TiC-coated diamond particles is denoted as TiC@diamond/Al. Meanwhile, the diamond particles without TiC coating were also used to produce a composite, denoted as Diamond/Al.

X-ray analysis was conducted on a D/max 2500PC diffractometer at 50 kV and 250 mA, using  $\text{Cu-K}\alpha$  radiation. The nitrogen content of the diamond was analyzed by LECO TCH 600. The diamond particles were observed by scanning electron microscopy (SEM, Supper 55). The TiC coatings on the diamond particles were analyzed by transmission electron microscopy (TEM, Tecnai F20, 200 KV) and high resolution TEM (HRTEM, Tecnai F20, 200 KV).

The thermal diffusivity of the composites was measured by a laser flash method (NETZSCH LFA447, Germany). The composites were cut to disk-shaped specimens 3 mm in thickness and 12.7 mm in diameter. The specific heat was measured by differential scanning calorimetry (DSC; NETZSCH STA 499 C, Germany). The specimens were machined into a disk shape 1 mm in thickness and 4 mm in diameter. The density was measured by the Archimedes method. The thermal conductivity was calculated as a product of thermal diffusivity, specific heat and density. The results are the average value of three tests in all cases and the standard errors are smaller than  $\pm 2\%$ .

To analyze the TiC coatings, the diamond particles were crashed and the TEM specimens were gained by copper grid. The TiC coatings were observed on the edge of the broken particles. The microstructure of the composites was analyzed by SEM. The SEM specimens were first polished by dimpling grinder which was usually used for the preparation of TEM specimens. Finally, the specimens were polished by ion beam (Leica EM RES101). The interfaces between the diamond and Al matrix were examined by TEM and HRTEM. Thin foils for TEM were machined by dimpling grinder using Buehler diamond paste (40–6246) and then thinned by ion milling.

The bending specimens were machined to a cuboid shape with dimensions of  $4 \times 4 \times 30 \text{ mm}^3$ . The fracture surfaces of the bending specimens were observed by SEM (Supper 55).

## 3. Results and discussion

Fig. 1 shows the XRD pattern of the diamonds. For the as-received diamond particles (Fig. 1a), there were no other peaks in the XRD pattern except diamond peaks. This indicates that there was no impurity in the diamond particles. For the TiC-coated diamond particles, the peaks of cubic TiC were observed in the XRD pattern and no other compounds were detected.

Fig. 2a shows the SEM images of the as-received diamond particles. The long and short axes of the diamond particles were about 70–80  $\mu\text{m}$  and 40–50  $\mu\text{m}$  in length, respectively. The low

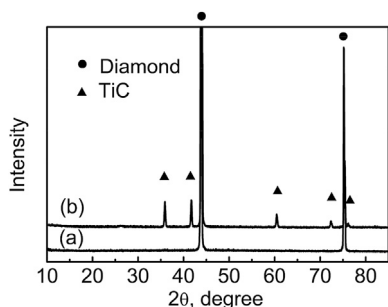


Fig. 1. XRD patterns of (a) as-received diamond and (b) TiC-coated diamond.

electroconductivity of the diamonds caused some particles to be very bright under SEM. Fig. 2b shows the SEM images of the TiC-coated diamond particles. The TiC-coated diamond particles were clean and the SEM image was very clear.

Fig. 2c shows the SEM image of the crashed TiC-coated diamond particles. The grey regions are the cleavage plane of the diamond particle, whereas the black region is the coating. It is noted that continuous and homogenous TiC coating was formed on the surface of the diamond particles. Fig. 2d shows a magnified image of the region marked by the white square in Fig. 2c. It is clear that the coating, composed of flat nanoparticles, was homogenous and integrated. It is different from the results of Tan et al. who achieved discontinuous W nanoparticles on the surface of diamond particles using the sol-gel method [19]. It is believed that the difference in the composite components and the manufacturing processes between two investigations result in the diversity of the two coatings.

Fig. 3a shows the TEM image of the edge of the crashed TiC-coated diamond particles. An integrated coating about 10 nm in thickness was clearly observed on the surface of the diamond particles. The coating was confirmed to be TiC by the HRTEM image,

shown in Fig. 3b. In order to confirm the lattice orientation relationship between diamond and coating intuitively and clearly, Fast Fourier Transform (FFT) was carried out to analyze the nanostructure with Digital Micrograph. Fig. 3b shows the FFT of diamond, coating, and the interface between diamond and coating. Clearly, the coating is cubic TiC, which is consistent with the above XRD analysis. Moreover, an orientation relationship between diamond and TiC coating  $(\bar{1}\bar{1}\bar{1})_{\text{TiC}}//(\bar{1}\bar{1}\bar{1})_{\text{Diamond}}$  and  $[110]_{\text{TiC}}//[110]_{\text{Diamond}}$  was observed, while the mismatch between the interplanar spacing of  $(\bar{1}\bar{1}\bar{1})_{\text{TiC}}$  (0.2492 nm) and  $(\bar{1}\bar{1}\bar{1})_{\text{Diamond}}$  (0.2059 nm) was about 17%.

Table 1 lists the density of the Diamond/Al and TiC@diamond/Al composites. While the density of the Diamond/Al was only 96.7% of the theoretical value, the density of the TiC@diamond/Al reached 99.6% of the theoretical value. Fig. 4a is the SEM image of the Diamond/Al. The black particles are the diamond particles and the grey regions are the Al matrix. There was no aggregation of diamond particles in the composites. However, some pores were observed at the interface of the diamond particles and Al matrix, indicated by the white arrows. This is consistent with the low density of the Diamond/Al, as shown in Table 1. Fig. 4b shows the SEM image of the TiC@diamond/Al. The microstructure is similar to that of the Diamond/Al. However, no pores were observed at the interface between diamond and Al matrix for the TiC@diamond/Al, indicating a good bonding between diamond and Al matrix. This is consistent with the high density of the TiC@diamond/Al (Table 1).

Fig. 5a shows the TEM image of the TiC@diamond/Al. Some dislocations were observed in the Al matrix near the interface due to the thermal expansion mismatch between the diamond particles and Al matrix, which is similar to the previous study [23]. At the interface between Al matrix and diamond, there was no TiC interlayer or other reaction product compounds. For all samples investigated in this study, no interlayer could be found at the interface between Al matrix and diamond.

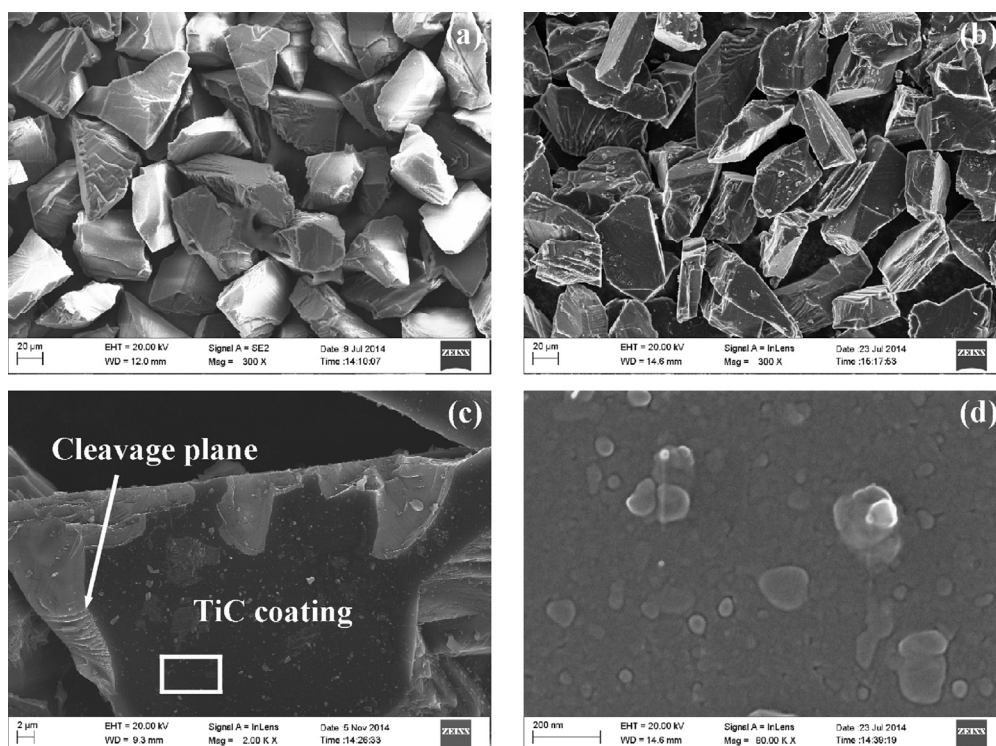


Fig. 2. SEM images of (a) as-received diamond, and (b) TiC-coated diamond, (c) crashed TiC-coated diamond, (d) magnified white square region in c.

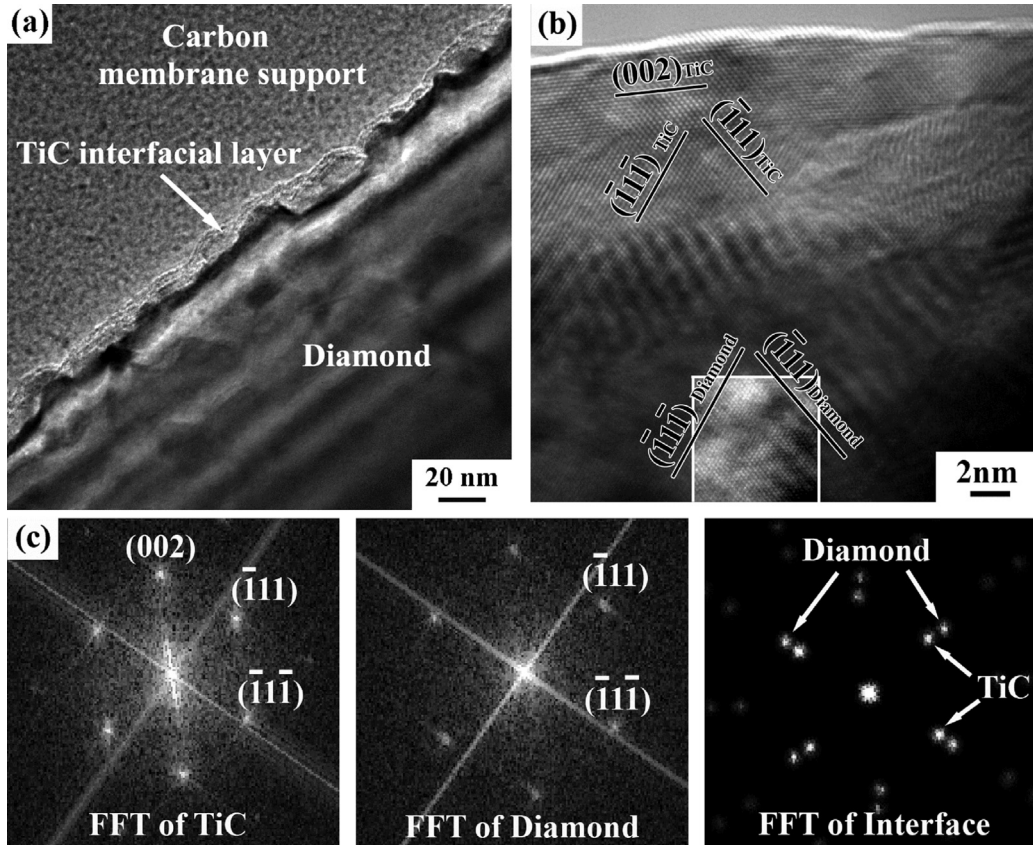


Fig. 3. Microstructure of TiC coating on diamond surface: (a) TEM image of TiC coating, (b) HRTEM image of TiC coating and (c) FFT of (b).

**Table 1**  
Density and properties of diamond/Al composites.

Materials	Density kg/m <sup>3</sup>	Bending strength MPa	TC W/mK
Diamond/6061Al	96.7% ± 0.1	294 ± 10	337 ± 1
TiC@diamond/6061Al	99.6% ± 0.1	396 ± 8	382 ± 1

Fig. 5b shows the HRTEM image of the interface. The FFT image of the Al/diamond interface is shown at the top-right corner in Fig. 5b. Due to the same lattice direction and small mismatch between the (020)<sub>Al</sub> (0.2025 nm) and (111)<sub>Diamond</sub> (0.2059 nm), the patterns of (020)<sub>Al</sub> and (111)<sub>Diamond</sub> seem to be elongated. Moreover, since the transmission electron beam is parallel to the

direction of [200]<sub>Al</sub> and [110]<sub>diamond</sub>, respectively, a crystallographic orientation relationship between Al matrix and diamond, (020)<sub>Al</sub>//(111)<sub>Diamond</sub> and [200]<sub>Al</sub>//[110]<sub>Diamond</sub>, could be observed. The mismatch between (020)<sub>Al</sub> and (111)<sub>Diamond</sub> is about 1.65%. It is well known a small lattice mismatch means a good bonding strength. No TiC was observed on the interface between diamond and Al matrix.

The thickness of the TiC coating on the diamond surface was very thin, only ~10 nm. It is assumed that the diamond particles are ellipsoids with a = b = 45 μm and c = 75 μm (as shown in Fig. 2) and the TiC is homogeneously distributed on the particle surface. Thus, the volume content of the TiC coating in the diamond particles is less than 0.058 vol%. For the composite reinforced with 50 vol% TiC-coated diamond, the content of the TiC in the composites was about 0.045 wt%. Correspondingly, the content of carbon which

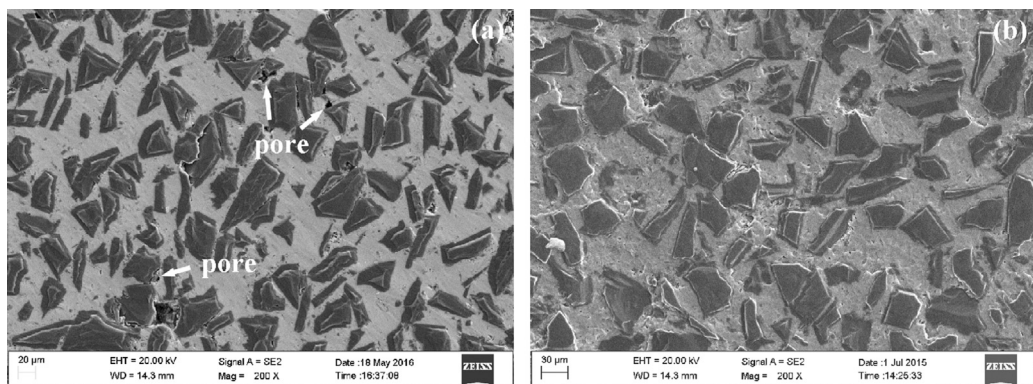


Fig. 4. SEM image of (a) Diamond/Al and (b) TiC@diamond/Al composites.

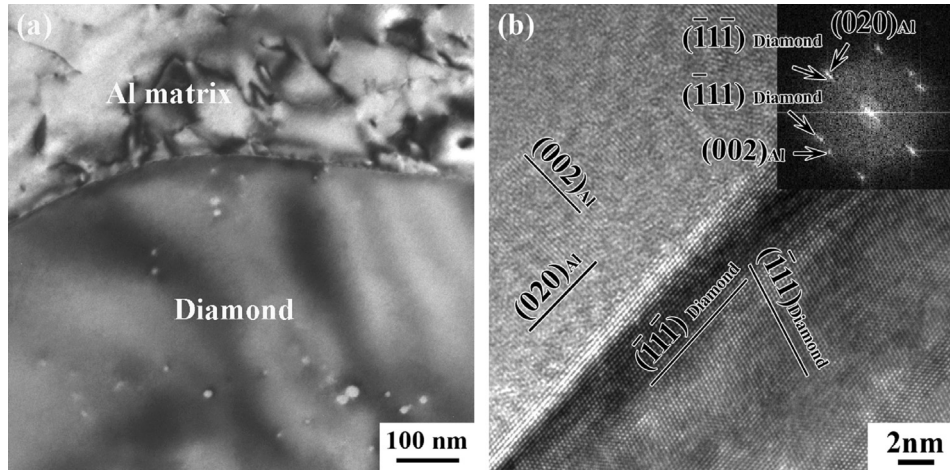


Fig. 5. (a) TEM image and (b) HRTEM image showing interface between diamond and Al matrix in TiC@diamond/Al composite.

originated from the TiC coating is only tens of ppm. According to a previous study on the phase equilibrium in the Al–Ti–C system [24], the Al–Ti–C solution could exist when the carbon content was very low. In this study, the low content of TiC and the high contact surface area between Al matrix and TiC would result in the dissolution of the TiC coating into the Al matrix during of the manufacture process of the composites at high temperature.

Table 1 shows the bending strength of the two composites. The strength of the TiC@diamond/Al was 396 MPa, which was increased by 35% compared to that of the Diamond/Al. Fig. 6a and b shows the SEM micrograph of the bending fracture surface of the Diamond/Al and the opposite fractograph of the same site, respectively. The grey particles were diamond and the other part with small dimples was the Al matrix. It is noted that most surfaces of the diamond particles were smooth on the fracture surface. This indicates that the diamond particles de-bonded with the Al matrix during the bending process.

The typical de-bonded particles are marked as No. 1 and 2 on the fracture surface of the TiC@diamond/Al (Fig. 6a and b). The poor wettability between the Al matrix and the diamond resulted in a weak interface bonding [19,25]. Therefore, the bending strength of the Diamond/Al was low. Furthermore, on the fracture surface, some pores were observed on the diamond particle edges, marked as No. 3 and 4. During the PM process, a small amount of liquid phase was formed. During the solidification process, the poor wettability between the Al matrix and the diamond would lead to the formation of voids at the interface. Therefore, the density of the composite was only 96.7% of the theoretical value. The low density decreased the bending strength of the composite.

Fig. 6c and d shows the micrograph of the bending fracture surface of the TiC@diamond/Al and the opposite fractograph of the same site, respectively. Obvious dimples were observed on the fracture surface. It is noted that nearly all diamond particles on the fracture surface were broken. The typical fractured particles are

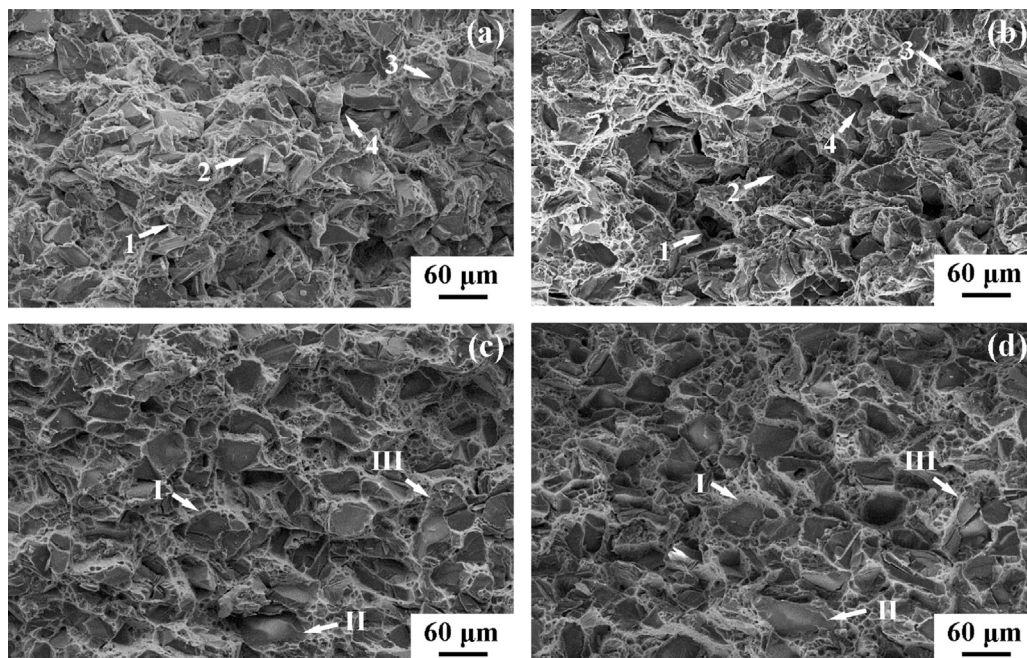


Fig. 6. SEM micrograph of bending fracture surface: (a) Diamond/Al, (b) opposite site of a, (c) TiC@diamond/Al, (d) opposite site of c.

marked as No. I, II and III in Fig. 6c and d. There were no pores on the fracture surface. The TiC coating could improve the wettability between the Al matrix and the diamond effectively. Although the TiC dissolved into the Al matrix, the interface bonding could be considerably increased. Therefore, the density and the bending strength of the composite were significantly increased, as shown in Table 1.

Table 1 shows the TC of the composites. The TC of the Diamond/Al was only 337 W/mK. The low density, especially the pores at the interface between the diamond particles and the Al matrix, would decrease the TC. For the TiC@diamond/Al, the TC was 382 W/mK, which was only a 13.4% increase compared to that of the Diamond/Al. Although the density of the TiC@diamond/Al was close to the theoretical value and the diamond and Al matrix had good bonding, the TC of the composite was still lower than previously reported values for the diamond/Al composites [10,16].

The low content (50 vol%) and the small size of the diamond particles in this study may be the main reason for this phenomenon. To remove the effect of particle size and content, the interfacial thermal conductance ( $h_c$ ) was usually used to evaluate the composites [26,27]. In this study, the diamond particles were assumed to be ellipsoids, not the spheres described in the previous reports [26,27]. Meanwhile, the diamond particles were randomly distributed (in Fig. 4). The Maxwell–Garnett type effective medium approximation (MG-EMA) model for ellipsoidal particle composites is applied to derive the  $h_c$  [28–30], which has been proven to be effective for the composites. In this model, when the ellipsoidal particles exhibit completely random distribution, the effective thermal conductivity  $K^*$  of the composites is expressed as [29].

$$K^* = K_m \frac{3 + f(2\beta_{11}(1 - L_{11}) + \beta_{33}(1 - L_{33}))}{3 - f(2\beta_{11}L_{11} + \beta_{33}L_{33})} \quad (1)$$

$$L_{11} = L_{22} = \frac{p^2}{2(p^2 - 1)} - \frac{p}{2(p^2 - 1)^{3/2}} \cosh^{-1} p \quad (2)$$

$$L_{33} = 1 - 2L_{11} \quad (3)$$

where  $p = a_3/a_1$  is the aspect ratio of the ellipsoid,  $a_3$  is the long axis radius of the ellipsoid, and  $a_1$  is the short axis radius of the ellipsoid.

where

$$\beta_{ii} = \frac{K_{ii}^c - K_m}{K_m + L_{ii}(K_{ii}^c - K_m)} \quad (4)$$

$$K_{ii}^c = K_p / (1 + \gamma L_{ii} K_p / K_m) \quad (5)$$

with

$$\gamma = (2 + 1/p)\alpha \quad (6)$$

where  $\alpha$  is defined by

$$\alpha = a_k/a_1 \quad a_k = R_{Bd}K_m \quad (7)$$

where  $K_m$  is the thermal conductivity of the matrix phase,  $K_p$  is the

thermal conductivity of diamond, and  $f$  is the particle volume fraction.

The nitrogen content of diamond was determined by analysis of its combustion product, yielding a nitrogen content of 100 ppm. Based on the data of Yamamoto [6], the intrinsic thermal conductivity of diamond in this work was assumed to be 1800 W/mK. For 6061 Al alloy, the  $K_m$  is 180 W/mK [31]. The  $h_c$  of the Diamond/Al was calculated to be  $3.4 \times 10^7$  W/m<sup>2</sup>K. By comparison, the  $h_c$  of the TiC@diamond/Al was  $5.22 \times 10^7$  W/m<sup>2</sup>K, raised up by 54% compared to that of the Diamond/Al. This indicates that the improvement of wettability of the interface between diamond and Al matrix could increase the  $h_c$  of the composites effectively.

As shown in Fig. 6, the TiC coating dissolved into the Al matrix and the diamond particles directly contacted with the Al matrix. The sharp interface could increase the phonon scattering, and therefore influence the coupling between diamond and Al matrix. The interfacial thermal conductance could be estimated by the acoustic mismatch model (AMM) [18,19,31]:

$$h \approx \frac{1}{2} \rho_m c_m \frac{v_m^3}{v_r^2} \frac{\rho_m v_m \rho_r v_r}{(\rho_m v_m + \rho_r v_r)^2} \quad (8)$$

where  $\rho$ ,  $c$ ,  $v$  are the mass density, the specific heat capacity and the phonon velocity, respectively. The subscripts  $c$ ,  $m$  and  $p$  refer to the composite, matrix and reinforcing particles, respectively.

The  $h_c$  between diamond and Al for the Diamond/Al was also calculated by the AMM. The relevant parameters of the materials used for the calculation are tabulated in Table 2. Due to the lack of data for 6061Al, the specific heat capacity and phonon velocity were substituted by those of the pure Al [19]. The  $h_c$  calculated by the AMM is  $4.5 \times 10^7$  W/m<sup>2</sup>K, similar to that of the TiC@diamond/Al derived by the MG-EMA model using experimental data.

As discussed above, the TiC coating improved the density of the composites from 96.7% to 99.6% of the theoretical value. Moreover, the TiC layer could promote bonding between the diamond particles and the Al matrix, facilitating the achievement of high strength in the TiC@diamond/Al. However, the thermal conductance of the TiC@diamond/Al only increased by 13.4% compared to that of the Diamond/Al. This means that the pores in the composites were not a key factor influencing the thermal conductance of the diamond reinforced Al composites.

The nanometer scale TiC layer dissolved into the Al matrix in the TiC@diamond/Al (shown in Fig. 5). The  $h_c$  between diamond and Al matrix of the TiC@diamond/Al (calculated by the MG-EMA model) was close to the theoretical value (calculated by the AMM). This indicates that the massive gap of the phonon velocity between diamond and Al, not the pores in the composites, was the major influence on the thermal conductance of the diamond particles reinforced Al composites.

#### 4. Conclusions

1. The TiC coating 10 nm in thickness on the diamond particles could improve the wettability between the diamond and Al matrix effectively. The density of the TiC@diamond/Al was 99.6% of the theoretical value compared to that of the Diamond/Al (only 96.7% of the theoretical value).

**Table 2**  
Parameters of materials for AMM model [20,32].

Materials	Density kg/m <sup>3</sup>	TC W/mK	Specific heat J/KgK	Phonon velocity m/s
Diamond	3500	1800	512	13,430
Al	2700	180	895	3620

2. The nanometer scale TiC coating improved the bonding between diamond particles and Al matrix. The bending strength of the TiC@diamond/Al was 396 MPa, which was 35% higher compared to that of the Diamond/Al.
3. The thermal conductance of the TiC@diamond/Al was only 13.4% greater than that of the Diamond/Al. The effect of the pores on the thermal conductance of the composites was not very obvious. The massive gap of the phonon velocity between diamond and Al influences the thermal conductance of the composites significantly.

### Acknowledgments

The authors gratefully acknowledge the support of the National Basic Research Program of China under Grant No. 2012CB619600 and the National Natural Science Foundation of China (Grant No. 51271051).

### References

- [1] A.M. Abyzov, S.V. Kidalov, F.M. Shakhov, High thermal conductivity composite of diamond particles with tungsten coating in a copper matrix for heat sink application, *Appl. Therm. Eng.* 48 (2012) 72–80.
- [2] M. Schobel, H.P. Degischer, S. Vaucher, M. Hofmann, P. Cloetens, Reinforcement architectures and thermal fatigue in diamond particle-reinforced aluminum, *Acta Mater.* 58 (2010) 6421–6430.
- [3] S. Rawal, Metal-matrix composites for space applications, *JOM* 53 (2001) 14–17.
- [4] J.D. Mathias, P.M. Geffroy, J.F. Silvain, Architectural optimization for micro-electronic packaging, *Appl. Therm. Eng.* 29 (2009) 2391–2395.
- [5] C. Xue, J.K. Yu, Enhanced thermal transfer and bending strength of SiC/Al composite with controlled interfacial reaction, *Mater. Des.* 53 (2014) 74–78.
- [6] Y. Yamanoto, T. Imar, K. Tanabe, T. Tsuno, Y. Kumazawa, N. Fujimori, The measurement of thermal properties of diamond, *Diam. Relat. Mater.* 6 (1997) 1057–1061.
- [7] K. Mizuuchi, K. Inoue, Y. Agari, Y. Morisada, M. Sugioka, M. Tanaka, et al., Processing of diamond particle dispersed aluminum matrix composites in continuous solid–liquid co-existent state by SPS and their thermal properties, *Compos Part B* 42 (2011) 825–831.
- [8] O. Beffort, F.A. Khalid, L. Weber, P. Ruch, U.E. Klotz, S. Meier, et al., Interface formation in infiltrated Al(Si)/diamond composites, *Diam. Relat. Mater.* 15 (2006) 1250–1260.
- [9] Y. Zhang, J.W. Li, L.L. Zhao, H.L. Zhang, X.T. Wang, Effect of metalloid silicon addition on densification, microstructure and thermal-physical properties of Al/diamond composites by spark plasma sintering, *Mater. Des.* 63 (2014) 838–847.
- [10] K. Chu, C.H. Jia, X.B. Liang, H. Chen, Effect of powder mixing process on the microstructure and thermal conductivity of Al/diamond composites fabricated by spark plasma sintering, *Rare Met.* 29 (2010) 86–91.
- [11] Z.Q. Tan, Z.Q. Li, G.L. Fan, X.H. Kai, G. Ji, L.T. Zhang, et al., Diamond/aluminum composites processed by vacuum hot pressing: microstructure characteristics and thermal properties, *Diam. Relat. Mater.* 31 (2013) 1–5.
- [12] H. Asgharzadeh, A. Simchi, Supersolidus liquid phase sintering of Al6061/SiC metal matrix composites, *Powder Metall.* 52 (2009) 28–35.
- [13] M. Schobel, G. Requena, G. Fiedler, D. Tolnai, S. Vaucher, H.P. Degischer, Void formation in metal matrix composites by solidification and shrinkage of an AlSi7 matrix densely packed particles, *Compos Part A* 66 (2014) 103–108.
- [14] N. Chen, C.F. Pan, M.Y. Gu, Microstructure and physical properties of Al/diamond composite fabricated by pressureless infiltration, *Mater. Sci. Tech.* 25 (2009) 400–402.
- [15] J.H. Wu, H.L. Zhang, Y. Zhang, J.W. Li, X.T. Wang, Effect of copper content on the thermal conductivity and thermal expansion of Al-Cu/diamond composites, *Mater. Des.* 39 (2012) 87–92.
- [16] Y. Zhang, J.W. Li, L.L. Zhao, X.T. Wang, Optimization of high thermal conductivity Al/diamond composites produced by gas pressure infiltration by controlling infiltration temperature and pressure, *J. Mater. Sci.* 50 (2015) 688–696.
- [17] H. Feng, J.K. Yu, W. Tan, Microstructure and thermal properties of diamond/aluminum composites with TiC coating on diamond particles, *Mater. Chem. Phys.* 124 (2010) 851–855.
- [18] K. Chu, Z.F. Liu, C.C. Jia, H. Chen, X.B. Liang, W.J. Gao, et al., Thermal conductivity of SPS consolidated Cu/diamond composites with Cr-coated diamond particles, *J. Alloy Compd.* 490 (2010) 453–458.
- [19] Z.Q. Tan, Z.Q. Li, G.L. Fan, Q. Guo, X.Z. Kai, G. Ji, et al., Enhanced thermal conductivity in diamond/aluminum composites with a tungsten interface nanolayer, *Mater. Des.* 47 (2013) 160–166.
- [20] C. Monachon, L. Weber, Thermal boundary conductance between refractory metal carbides and diamond, *Acta Mater.* 73 (2014) 337–346.
- [21] C. Xue, J.K. Yu, Enhanced thermal conductivity in diamond/aluminum composites: comparison between the methods of adding Ti into Al matrix and coating Ti onto diamond surface, *Surf. Coat. Technol.* 217 (2013) 46–50.
- [22] A.R. Kennedy, S.M. Wyatt, Characterising particle–matrix interfacial bonding in particulate Al-TiC MMCs produced by different methods, *Compos Part A* 32 (2001) 555–559.
- [23] G. Ji, Z.Q. Tan, R. Shabadi, Z.Q. Li, W.G. Grünwald, A. Addad, et al., Triple ion beam cutting of diamond/Al composites for interface characterization, *Mater. Charact.* 89 (2014) 132–137.
- [24] N. Frage, M. Polak, M.P. Dariel, N. Frumin, L. Levin, High-temperature phase equilibria in the Al-rich corner of the Al-Ti-C system, *Metall. Mater. Trans. A* 29 (1998) 1341–1345.
- [25] K.A. Weidenmann, R. Tavangar, L. Weber, Mechanical behaviour of diamond reinforced metals, *Mater. Sci. Eng. A* 523 (2009) 226–234.
- [26] G. Justyna, J.K. Miroslaw, K. Marcin, C. Lukasz, M. Andrzej, J.K. Krzysztof, Interfacial microstructure of copper/diamond composites fabricated via a powder metallurgical route, *Mater. Charact.* 99 (2015) 188–194.
- [27] Y. Zhang, H.L. Zhang, J.H. Wu, X.T. Wang, Enhanced thermal conductivity in copper matrix composites reinforced with titanium-coated diamond particles, *Scr. Mater.* 65 (2011) 1097–1100.
- [28] H.L. Duan, B.L. Karihaloo, Effective thermal conductivities of heterogeneous media containing multiple imperfectly bonded inclusions, *Phys. Rev. B* 75 (2007), 064206–1–9.
- [29] C.W. Nan, R. Birringer, D.R. Clarke, H.H.L. Gleiter, B.L. Karihaloo, Effective thermal conductivity of particulate composites with interfacial thermal resistance, *J. Appl. Phys.* 81 (1997) 6692–6699.
- [30] H.L. Duan, M. Taya, The effective thermal conductivity of composites with coated reinforcement and the application to imperfect interfaces, *J. Appl. Phys.* 73 (1993) 1711–1722.
- [31] Aerospace structural metals database. <http://cindasdata.com/Applications/ASMD/?subaction=reload%3Amcode&mname=2124&mcode=3221>.
- [32] K. Chu, C.C. Jia, X.B. Liang, H. Chen, W.J. Gao, H. Guo, Modeling the thermal conductivity of diamond reinforced aluminum matrix composites with inhomogeneous interfacial conductance, *Mater. Des.* 30 (2009) 4311–4316.